AIP | Applied Physics Letters

Fabrication of submicron structures in nanoparticle/polymer composite by holographic lithography and reactive ion etching

A. Ping Zhang, Sailing He, Kyoung Tae Kim, Yong-Kyu Yoon, Ryszard Burzynski, Marek Samoc, and Paras N. Prasad

Citation: Applied Physics Letters **93**, 203509 (2008); doi: 10.1063/1.2998541
View online: http://dx.doi.org/10.1063/1.2998541
View Table of Contents: http://scitation.aip.org/content/aip/journal/apl/93/20?ver=pdfcov
Published by the AIP Publishing

Fabrication of submicron structures in nanoparticle/polymer composite by holographic lithography and reactive ion etching

A. Ping Zhang,[1] Sailing He,[1] Kyoung Tae Kim,[2] Yong-Kyu Yoon,[2] Ryszard Burzynski,[3] Marek Samoc,[4,5] and Paras N. Prasad[4,a)]
[1]*Centre for Optical and Electromagnetic Research, Department of Optical Engineering, Zhejiang University, Hangzhou 310058, People's Republic of China*
[2]*Department of Electrical Engineering, State University of New York at Buffalo, Buffalo, New York 14260, USA*
[3]*Laser Photonics Technology, Inc., 1576 Sweet Home Rd., Amherst, New York 14228, USA*
[4]*Institute for Lasers, Photonics and Biophotonics, State University of New York at Buffalo, Buffalo, New York 14260, USA*
[5]*Laser Physics Centre, Australian National University, Canberra, ACT 0200, Australia*

(Received 28 May 2008; accepted 9 September 2008; published online 20 November 2008)

We report on the fabrication of nanoparticle/polymer submicron structures by combining holographic lithography and reactive ion etching. Silica nanoparticles are uniformly dispersed in a (SU8) polymer matrix at a high concentration, and *in situ* polymerization (cross-linking) is used to form a nanoparticle/polymer composite. Another photosensitive SU8 layer cast upon the nanoparticle/SU8 composite layer is structured through holographic lithography, whose pattern is finally transferred to the nanoparticle/SU8 layer by the reactive ion etching process. Honeycomb structures in a submicron scale are experimentally realized in the nanoparticle/SU8 composite. © *2008 American Institute of Physics*. [DOI: 10.1063/1.2998541]

Nanoparticles have an enabling role in various branches of nanotechnology due to their capability of being a bridge between bulk materials and atomic or molecular structures.[1,2] Recently, composite materials made of polymers and nanoparticles have attracted great attention because of the stabilizing effects of the composite on the nanoparticle functionalities[3,4] and relative easiness and flexibility of engineering composites with advanced electrical, optical, or mechanical properties.[5,6] On the other hand, submicron-scale periodic structures are essential for the applications such as photonic or optoelectronic devices[7,8] and biochemical sensors.[9] For instance, photons can be controlled through the band gap of photonic crystals, which requires photonic materials to be periodically structured on a length scale comparable to that of the wavelength of light (i.e., the submicron range for the optical domain). Therefore, there is a need for an efficient approach to patterning nanoparticle/polymer composites into periodically ordered structures. Although various fabrication approaches were developed for microfabrication of polymeric devices[10,11] or precise arrangement of nanoparticles into patterns,[12] the patterning of nanoparticle/polymer composites necessitates special consideration due to quite often great differences in mechanical and optical properties of their constituents. A practical solution is to adopt a two-step fabrication scheme with separated pattern definition and pattern transfer procedures. Several well-developed techniques can be used for such a fabrication scheme. The objective pattern can be defined by interference lithography,[13] or nanosphere lithography,[14,15] and reactive ion etching (RIE)[15] or electrodeposition,[16] can perform the pattern transfer. Among various technologies, the fabrication based on interference lithography has attracted a great deal of attention due to its capability of rapidly producing large-area microstructures. It was demonstrated that self-assembled nanoparticles could be patterned over a large area by combining two-beam interference lithography and the RIE process.[17] In this letter, we apply this technology to pattern a nanoparticle/polymer composite in which holographic lithography (HL) based on three-beam interference process is utilized to tailor the geometry of microstructures, and RIE is used to create the nanostructured patterns.

The materials chosen for this investigation are Epon SU8 photoresist and colloidal silica nanoparticles (SNP). SU8 is an excellent photoresist for laser patterning, and it has been utilized as a permanent structural material for micro- and nanotechnologies, e.g., microelectromechanical systems[18] or microfluidic devices,[19] because of its good chemical and biochemical compatibilities.

Figure 1 shows the scheme of pattern formation by HL in the top (lithography) layer and its transfer by RIE to the bottom (nanoparticle/polymer composite) layer. The colloidal SNPs are mixed with SU8 solution and spin coated on the glass substrate. After polymerization, another photosensitive SU8 layer is casted on the top of the first layer for HL. The structures created by the HL are used as a seed pattern (or mask), which is then transferred to the bottom layer by the RIE process. Since SU8 can be effectively etched by oxygen plasma,[20,21] one can simultaneously realize the pattern transfer and "mask" removal by properly designing film properties and process parameters. HL is employed to create such a large-area mask. Three noncoplanar laser beams interfere, as shown in Fig. 1(b), and create a stationary spatial variation in intensity, whose geometry can be tailored by varying polarization of the laser beams. Figures 1(c) and 1(d) show two typical configurations of beam polarizations and the corresponding two-dimensional structures that are created in a negative photoresist.

The commercial colloidal SNPs (Nissan Chemical, MEK-ST) used in the experiments have particle sizes of 10–15 nm, and are dispersed in methyl ethyl ketone with a weight ratio of 30%. They are added, together with a

a)Author to whom correspondence should be addressed. Electronic mail: pnprasad@buffalo.edu.

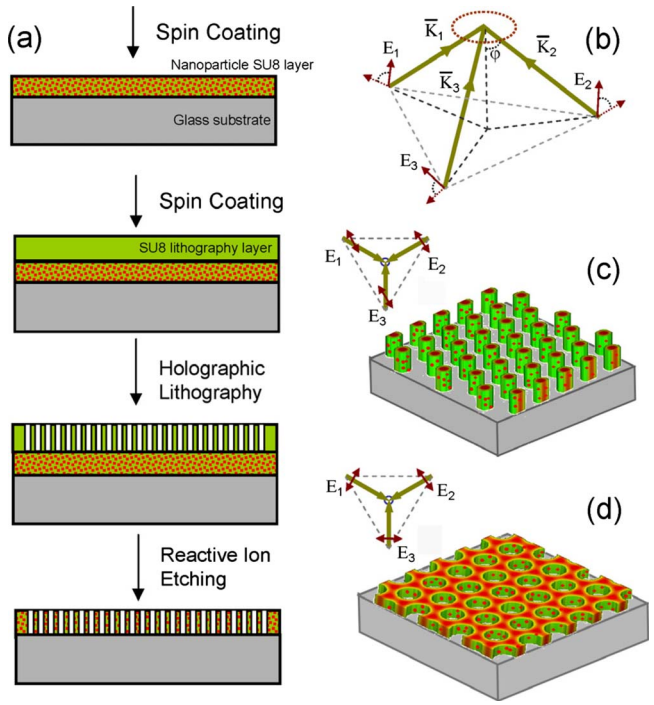

FIG. 1. (Color online) (a) The scheme for patterning of the nanoparticle/polymer composite film by HL and RIE. (b) Schematics of the laser beam configuration for HL and polarization configurations for (c) column structure and (d) air-hole structure.

small amount of a photoacid generator, into the SU8/cyclopentanone solution (weight ratio of 10%), and mixed using ultrasonic bath to obtain the nanoparticle-dispersed photoresist solution. This solution is spin coated on a glass substrate, and the solvent is removed by a soft bake at 95 °C. After flood exposure under a UV lamp for 5 min, the film is hard baked at 125 °C to achieve polymerization (cross-linking). Figure 2 shows the scanning electron microscopy (SEM) images of the surface of the nanoparticle/polymer film. In order to clearly show the surface of nanoparticles, a soft oxygen plasma process is applied before taking SEM images. One can see that the nanoparticles are uniformly distributed in the SU8 matrix, and there is no significant aggregation. The size of a polymer-coated nanoparticle is around 35–45 nm.

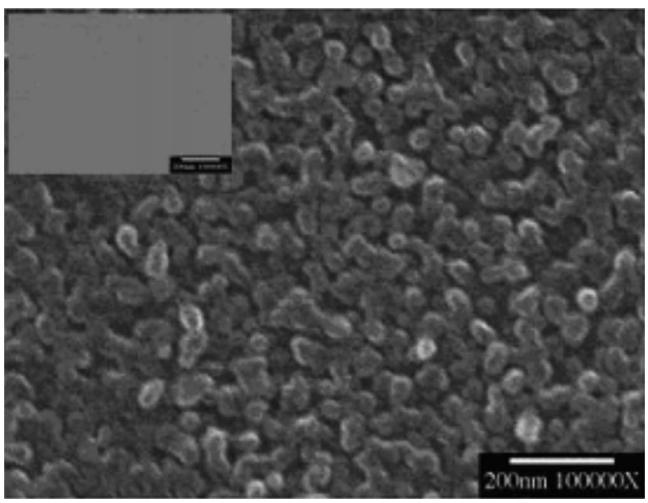

FIG. 2. SEM image showing the surface of the nanoparticle/polymer composite film after a soft oxygen-plasma process. The inset shows the surface of the film without the oxygen-plasma process.

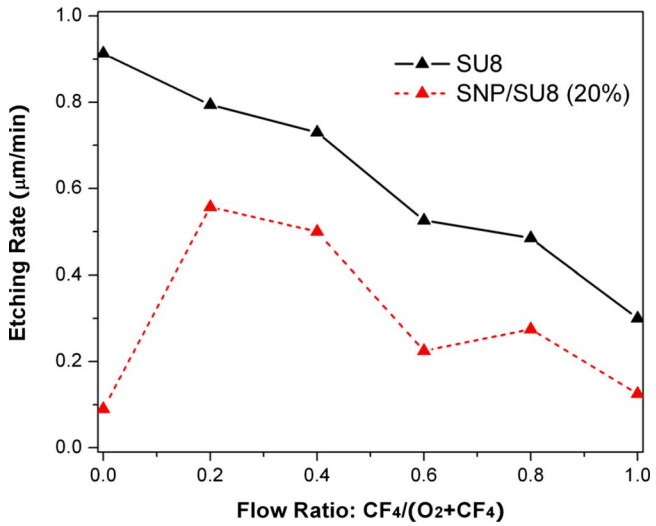

FIG. 3. (Color online) Etching rates of SU8 films (black solid line) and SNP/SU8 composite films (red dash line) as a function of the $CF_4/(O_2+CF_4)$ flow ratio.

In order to examine the effects of embedded SNPs on the process, we utilize the RIE process with O_2/CF_4 etching gas mixture and test the etching rates of the SU8 films containing SNPs. With a radio frequency (rf) power of 130 W and etching time of 1 min, the films are etched with different flow rates of the O_2/CF_4 gas mixture. Figure 3 shows the measured etching rates for different gas flow ratios (O_2/CF_4), namely, 16.5 SCCM (SCCM denotes cubic centimeter per minute at STP) /0.0 SCCM, 13.2 SCCM/3.3 SCCM, 9.9 SCCM/6.6 SCCM, 6.6 SCCM/9.9 SCCM, 3.3 SCCM/13.2 SCCM, and 0.0 SCCM/16.5 SCCM. Each data point of etching rate is obtained by averaging from two experiments. The data show that the pure SU8 film can be effectively etched by the oxygen plasma, and that the etching rate decreases with the increased content of CF_4 in the etchant gas mixture. The etching rate of SU8 in pure oxygen plasma is approximately 900 nm/min, which is about three times higher than the etching rate of SU8 in pure CF_4 plasma. After mixing SU8 with SNP (SNP/SU8=20 wt %), however, the etching rate in pure oxygen plasma becomes much lower (approximately 100 nm/min). It is mainly due to the inertness of SNP to the oxygen plasma. Adding a specific amount of CF_4 can increase the etching rate. As shown in Fig. 3, the fastest etching, at a rate of around 560 nm/min, is achieved when the etchant gas mixture is $O_2:CF_4=4:1$ (vol/vol).

In our experiments, visible light lithography is performed by using the output beam from a cw $Nd:YVO_4$ laser (Coherent, Verdi V6) operating at 532 nm. The material preparation and optical lithography processing are as presented before.[11] Figure 4 shows an example of SU8 microstructures fabricated by using the configuration of laser beams of Fig. 1(d). It is an air-hole structure with a triangular symmetry having a lattice constant of 700 nm. The incident angle for the laser beams (angle between the beam's **k** vector and the normal to the substrate in air) was set to be 30° in this fabrication.

In order to achieve simultaneous pattern transfer and mask removal, the thicknesses of the lithography layer and the nanoparticle/polymer layer can be optimized using the data presented in Fig. 3. It is noted that the etching rate of

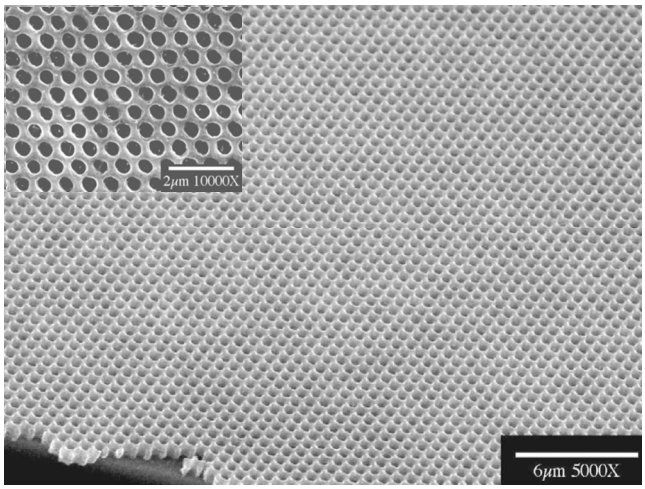

FIG. 4. (Color online) SEM image (off-angle view) showing the SU8 air-hole structure with a triangular symmetry created by HL. The inset shows the top view of the same sample.

RIE depends on the feature size of the structure, and the etching rate typically decreases when the feature size becomes smaller. The thickness of films fabricated by spin coating can be easily tailored by controlling the concentration of polymer solution and the spinning rate. In our experiments, the SU8 resin is dissolved in cyclopentanone at a concentration of 10 wt %, and spin coated on a glass substrate at the rate of 3500 rpm to achieve a thickness of the nanoparticle/polymer layer of approximately 200 nm. The SU8 solution for the lithography layer, however, has a concentration of 30 wt % and is spin coated on the nanoparticle/polymer layer with a speed of 2500 rpm to achieve a thickness of the photoresist layer of approximately 800 nm. After the HL process, the RIE process is applied to complete the patterning of nanoparticle/polymer film. The RIE process is preformed by using a bench-top RIE system (RIE-1C; SAMCO, Inc.). The etching parameters used are as follows: O_2 flow rate: 12.5 SCCM, CF_4 flow rate: 3.0 SCCM, rf power: 130 W, and etching time: 70 s.

Figure 5 shows the SEM images of the fabricated nanoparticle/polymer microstructure whose upper layers (masks) were fabricated by using different HL configurations. The fabricated air-hole structure is of triangular symmetry having a lattice constant of 500 nm (the incident angle for the laser beams is 45°). One can see that the nanoparticles are well ordered to form a submicron-scale honeycomb structure. The air-hole size becomes somewhat larger than the mask structure defined by HL due to the undercut issue.[22] The pattern transfer can be further improved if the RIE system could operate at a lower chamber pressure and temperature to improve directionality of the etching process.

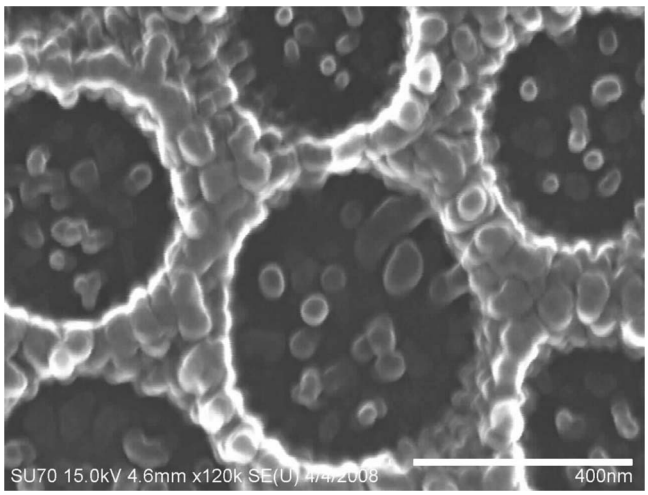

FIG. 5. SEM images showing the top view of the fabricated air-hole structure with a triangular symmetry.

The demonstrated fabrication procedure is powerful because the HL can flexibly define complex patterns and the RIE process can be designed for different materials. Good compatibility of HL and RIE processes is assured because the same polymer system is used for making the composite and the lithography films. This approach is therefore very promising for structuring semiconductor nanocrystals or quantum-dot doped polymer composites into advanced nanophotonic devices.

In conclusion, we have introduced a fabrication approach for patterning nanoparticle/polymer films by combining the HL and RIE processes. A fabrication process for SNP doped SU8 film has been established by using visible light lithography and the O_2/CF_4 gas mixture RIE process. Such a two-step fabrication scheme allows patterning of nanocomposites with high concentration of key components such as nanoparticles or quantum dots. The experimental results show the powerfulness of the approach for further exploring the utility of nanoparticle/polymer composites in photonic applications.

This work was supported in part by the US Air Force Office for Scientific Research and in part by National Basic Research Program (973) of China (No. 2004CB719800).

[1]G. Schmid, *Nanoparticles: From Theory to Application* (Wiley-VCH, Weinheim, 2004).
[2]A. P. Alivisatos, Science **271**, 933 (1996).
[3]J.-F. Berret, J. Phys. Chem. B **110**, 19140 (2006).
[4]R. B. Grubbs, Polym. Rev. **47**, 197 (2007).
[5]A. C. Balazs, T. Emrick, and T. P. Russell, Science **314**, 1107 (2006).
[6]S. Jiguet, A. Bertsch, M. Judelewicz, H. Hofmann, and P. Renaud, Microelectron. Eng. **83**, 1966 (2006).
[7]J. D. Joannopoulos, P. R. Villeneuve, and S.-H. Fan, Nature (London) **386**, 143 (1997).
[8]J. G. C. Veinot, H. Yan, S. M. Smith, J. Cui, Q. Huang, and T. J. Marks, Nano Lett. **2**, 333 (2002).
[9]E. Chow, A. Grot, L. W. Mirkarimi, M. Sigalas, and G. Girolami, Opt. Lett. **29**, 1093 (2004).
[10]S. Y. Chou and L. Zhuang, J. Vac. Sci. Technol. B **17**, 3197 (1999).
[11]A. P. Zhang, R. Burzynski, Y.-K. Yoon, P. N. Prasad, and S. He, Opt. Lett. **33**, 1303 (2008).
[12]A. Blaaderen, R. Ruel, and P. Wiltzius, Nature (London) **385**, 321 (1997).
[13]D. Xia and S. R. J. Brueck, Nano Lett. **4**, 1295 (2004).
[14]C. L. Haynes and R. P. V. Duyne, J. Phys. Chem. B **105**, 5599 (2001).
[15]D. Xia, Z. Ku, D. Li, and S. R. J. Breck, Chem. Mater. **20**, 1847 (2008).
[16]I. B. Divliansky, A. Shishido, I.-C. Khoo, and T. S. Mayer, Appl. Phys. Lett. **79**, 3392 (2001).
[17]D. Xia, L. Dong, Y. Luo, and S. R. J. Brueck, Adv. Mater. (Weinheim, Ger.) **18**, 930 (2006).
[18]P. Abgrall, V. Conedera, H. Camon, A.-M. Gue, and N.-T. Nguyen, Electrophoresis **28**, 4539 (2007).
[19]P. Abgrall and A.-M. Gue, J. Micromech. Microeng. **17**, R15 (2007).
[20]G. Hong, A. S. Holmes, and M. E. Heaton, Microsyst. Technol. **10**, 357 (2004).
[21]C.-H. Lee, T.-W. Chang, K.-L. Lee, J.-Y. Lin, and J. Wang, Appl. Phys. A: Mater. Sci. Process. **79**, 2027 (2004).
[22]S. Franssila, *Introduction to Microfabrication* (Wiley, Chichester, 2004), Chap. 11.